

**Top and bottom interfaces in Fe-B multilayers investigated by Mössbauer spectroscopy**

J. Balogh,\* L. Bujdosó, and D. Kaptás

*Institute for Solid State Physics and Optics, Wigner Research Centre for Physics, Hungarian Academy of Sciences,  
P.O. Box 49, 1525 Budapest, Hungary*

I. Dézsi

*Institute for Particle and Nuclear Physics, Wigner Research Centre for Physics, Hungarian Academy of Sciences,  
P.O. Box 49, 1525 Budapest, Hungary*

A. Nakanishi

*Department of Physics, Shiga University of Medical Science, Shiga 520-2192, Japan*

(Received 22 February 2012; revised manuscript received 26 April 2012; published 15 May 2012)

Mössbauer spectroscopy is frequently applied to gain information on the interfaces in multilayers, and recently the layer sequence permutation of multitrilayers was suggested to enhance its capability to characterize bottom and top interfaces of a given layer. The sequence permutation, however, in the investigated Fe-B-Ag multitrilayers affected the waviness of the layers as well, and the results hinted at the possibility that although Ag does not mix with Fe and B, the Fe-B amorphous alloy formation is influenced by the layer-sequence-dependent morphology of the Ag layers in the multitrilayers. Now we examine the interface mixing of Fe and B in the case of a fixed layer sequence and varying thickness of the Ag layers in  $[2 \text{ nm B}/2 \text{ nm Fe}/x \text{ nm Ag}]_4$ ,  $0.2 \leq x \leq 10$ , multitrilayer samples and in B/Fe/B and B/Fe/Ag trilayers. Below  $x = 5 \text{ nm}$ , both the ratio of the nonalloyed Fe layer and the average hyperfine field of the amorphous Fe-B interface compound change. The variation is attributed to thickness-dependent discontinuities of the Ag layers. Ag acts as a barrier to the diffusion of B from the top side and thus the discontinuities lead to a varying ratio of top and bottom interfaces. The evaluation based on this model shows that the “B on top of Fe” interface has an average B concentration about 11 at. % higher than the “Fe on top of B” interface. A slightly smaller difference, 6 at. %, is deduced from low-temperature conversion electron Mössbauer spectroscopy measurements of the trilayers.

DOI: [10.1103/PhysRevB.85.195429](https://doi.org/10.1103/PhysRevB.85.195429)

PACS number(s): 76.80.+y, 68.35.-p, 75.70.Cn

**I. INTRODUCTION**

Mössbauer spectroscopy (MS), which is sensitive to the local neighborhood of the Mössbauer isotope, is widely used to study nanoscale multilayers. The  $^{57}\text{Fe}$  marker method—in which the position of a thin  $^{57}\text{Fe}$  layer is varied across the natural Fe- or Fe-containing layer<sup>1–6</sup>—detected differences of the bottom and the top interface<sup>7–9</sup> in some multilayer structures. The application of the above method is, however, limited by the possible mixing and diffusion between the  $^{57}\text{Fe}$  and the natural Fe layers or the compound layers containing them.<sup>10,11</sup> A rarely used approach,<sup>12</sup> the sequence permutation of three building block multilayer structures (multitrilayers), was studied recently.<sup>13</sup> In order to distinguish the bottom and top interfaces of the Fe layer, a third element is interleaved, and the multitrilayers composed of three different elemental layers are deposited by sequence permutation in two different forms. In samples with a different layer sequence, each element pair has a different type interface; one of the elements is either on top or at the bottom of the other. The Fe-B multilayer system was chosen to be studied this way<sup>13</sup> because a significant mixing of the elements occurs at the interfaces during the sample deposition, which is accompanied by solid-state amorphization.<sup>14,15</sup> Ag was interleaved, as the third building block, since it does not mix with either of the other two elements: both Fe-Ag and B-Ag are nonmixing element pairs. A further advantage of the application of Ag is that the hyperfine fields of Fe at the Fe-Ag interfaces<sup>9,16–18</sup> can be rather well separated from those of the amorphous or

crystalline Fe-B alloys.<sup>13,19</sup> Analysis of the results obtained by MS for sequence-permuted sample pairs had shown<sup>13</sup> that the composition of the amorphous interfaces depends on the layer sequence; chemical mixing is larger when B is on top of the Fe layer.

The layer permutation, however, influenced the sample morphology to a large extent, as was revealed by transmission electron microscopy investigations.<sup>13</sup> Large interface roughness and waviness of the layers was observed when Ag was grown on top of the B layer, but B was found to grow on Ag smoothly. As a consequence, the variance of the Ag layer thickness was larger for the Fe/B/Ag than for the B/Fe/Ag sequence. The comparison of Mössbauer measurements on trilayer and multilayer samples suggested the possibility that the larger variance of the Ag layer thickness might also contribute to the observed enhanced B concentration of the “B on top of Fe” (Fe/B) interface in the case of the Fe/B/Ag layer sequence. In the present paper, we study in greater detail how the thickness of the Ag layers interleaved into Fe-B multilayers influences the chemical mixing of Fe and B. In view of the above-described morphological differences, the B/Fe/Ag sequence is chosen for the investigations.

Regardless of the sequence of the layers, the question can be raised whether the interleaved Ag layers affect the layer growth processes, and in this way the chemical mixing at the interfaces intended to be studied. For this reason, trilayer samples of B/Fe/B and B/Fe/Ag sequences over the Si substrate will be investigated using low-temperature conversion electron

Mössbauer spectroscopy (CEMS) measurements. Since the Ag capping layer is not supposed to affect the “Fe on top of B” (B/Fe) interface in the case of the second sample, the unperturbed Fe/B and B/Fe interfaces can be compared directly in this way. If these interfaces are equivalent, one will observe the same kind of interface component in the above two samples, and any difference observed beyond the spectral weight of the interface components will be indicative of the nonequivalent nature of these interfaces.

Investigation of multilayers offering new material properties for different applications<sup>20,21</sup> has an increasing importance, but experimental results on the properties of the interfaces in multilayers are scarce.<sup>22</sup> The effect of the layer sequence on the physical properties has been demonstrated in several trilayer studies,<sup>23–25</sup> and it was explained by a difference between the top and bottom interfaces. The simple approach presented in the following to examine this difference can be applied to a wide range of material combinations; the nonmixing nature of the interleaved element with both of the other two components is not a necessary requirement.

## II. EXPERIMENT

The samples were prepared by thermal evaporation in a high vacuum chamber with a base pressure of  $10^{-7}$  Pa onto Si(111) wafers at room temperature. Ag and B were evaporated from Cu cold crucibles by electron guns, and  $^{57}\text{Fe}$  was evaporated from a heated W boat. In the case of the multilayer samples, the first layer was always 5 nm Ag and the subsequent 16–56-nm-thick B/Fe/Ag multilayers were covered by 50 nm Ag and 100 nm B (cover in the following) in order to prevent the oxidation of the samples and to make them easily removable from the substrate. The layers removed were cut into smaller pieces and stacked to increase the measuring efficiency. The following multilayer samples were prepared:

(a) Si/5 nm Ag/[2 nm B/2 nm  $^{57}\text{Fe}/x$  nm Ag]<sub>4</sub>/cover, with  $x = 0.2, 0.4, 1, 2, 4, 5$ , and 10.

The bracket and the subscript to it indicate the multilayer unit and the number of repetitions, respectively. For the CEMS measurements, two samples were prepared:

(b) Si/5 nm B/2.5 nm  $^{57}\text{Fe}$ /5 nm B/10 nm Ag.

(c) Si/5 nm B/2.5 nm  $^{57}\text{Fe}$ /10 nm Ag.

Samples (b) and (c) were prepared parallel in such a way that all the layers, except the second B layer of sample (b), were evaporated together in a vacuum chamber with two substrate holders. The mass of the evaporated material was measured by a quartz oscillator and the nominal Ag layer thickness calculated from bulk density data showed a reasonable agreement with the Ag thickness observed by transmission electron microscopy in the case of the  $x = 5$  sample.<sup>13</sup> Due to the formation of the amorphous Fe-B interface alloy and the amorphous (nanocrystalline) nature of the nonalloyed B (Fe) layer, the results were not informative on the Fe and B layer thickness, but the presence of a continuous fcc-Ag layer with average thickness around 5 nm could be confirmed.

The transmission MS measurements were made with a 50 mCi  $^{57}\text{Co}$ -Rh source in a standard constant acceleration spectrometer. The low-temperature transmission measurements were performed in a cryostat attached to a closed-cycle refrigerator. CEMS spectra were measured at 15 K by a

$\text{H}_2$  filled proportional counter.<sup>26</sup> The hyperfine field (HF) distributions were evaluated according to the Hesse-Rübartsch method.<sup>27</sup> The isomer shift (IS) is given as relative to  $\alpha$ -Fe at room temperature.

## III. RESULTS AND DISCUSSION OF B/Fe/Ag MULTITRILAYER SAMPLES

Low-temperature Mössbauer spectra of a few selected samples are shown in Fig. 1(a). The spectrum for  $x = 0$  is in accordance with the results obtained earlier for Fe-B multilayers.<sup>14</sup> The 2 nm Fe layers are fully intermixed with B, and according to the fitted HF distribution, shown in Fig. 1(b), they form an amorphous alloy with a broad concentration distribution.

For  $x = 5$  and 10, the measured spectra agree within the experimental errors and can be described by a slightly broadened [ $\Gamma = 0.41(1)$  mm/s] sextet and a HF distribution, as indicated in Fig. 1(a) by the two subspectra. The sextet component [ $\text{HF} = 34.1(1)$  T,  $\text{IS} = 0.13(1)$  mm/s] can be attributed to the crystalline Fe layers. The slightly increased linewidth and HF as compared to those measured on bulk  $\alpha$ -Fe [ $\Gamma = 0.24(1)$  mm/s,  $\text{HF} = 33.8(1)$  T] can be due to the presence of an unresolved Fe/Ag interface component. The Fe/Ag interfaces are significantly narrower than the B/Fe

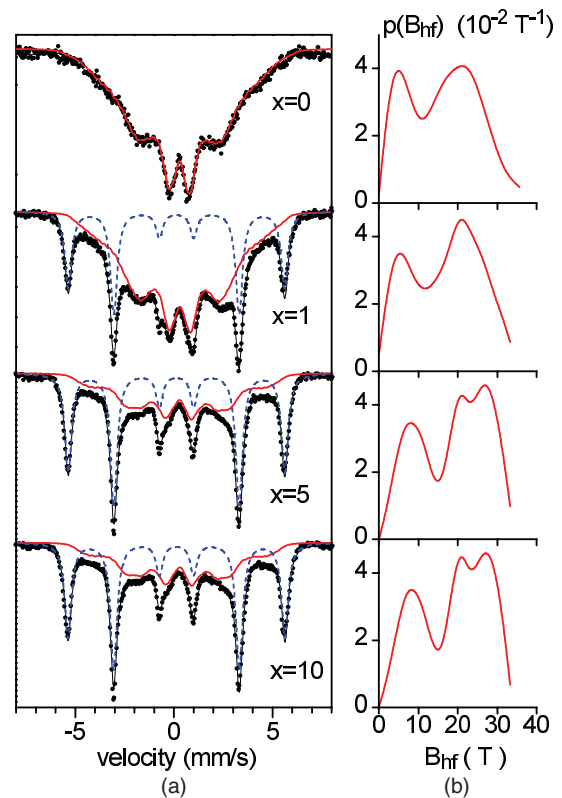


FIG. 1. (Color online) (a) Mössbauer spectra of a few selected samples of the [2 nm B/2 nm  $^{57}\text{Fe}/x$  nm Ag]<sub>4</sub> multilayer series measured at 13 K. The spectra were fitted by one sextet belonging to the crystalline Fe layer and a distribution of hyperfine fields describing the Fe-B interface, as indicated by dashed (blue) and full (red) lines, respectively. (b) Normalized hyperfine field distributions evaluated for the Fe-B interface component.

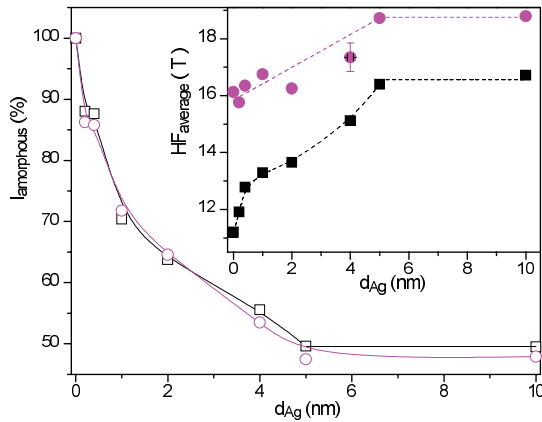


FIG. 2. (Color online) Spectral area (open symbols) and average HF (full symbols) of the fitted distribution at room (squares) and at 13 K (dots) temperatures as a function of the nominal Ag layer thickness. The lines are guide to the eye.

interfaces,<sup>13,28,29</sup> and beyond the broadening of the crystalline sextet they might contribute in a small extent to the high field components (above 30 T) of the HF distribution. The broad HF distribution with HF = 18.8(2) T and IS = 0.26(2) mm/s average values is attributed to the amorphous B/Fe interfaces.<sup>14</sup> According to the spectral areas, there are an approximately equal number of Fe atoms that belong to the amorphous B/Fe interface and to the crystalline Fe layer. [The HF distribution accounts for 46(5)% of the spectral area.] This means that on average, the thickness of the crystalline Fe layer is close to 1 nm and the amount of Fe atoms in the amorphous interface is also equivalent to a 1-nm-thick Fe layer. This conclusion is also supported by measurements on a series of B/Fe/Ag multilayer samples<sup>30</sup> with nominal Fe layer thickness fixed to 1 nm, where no crystalline sextet component was observed.

The variation of the spectral fraction of the amorphous interface and the average HF value of the amorphous component as a function of the Ag layer thickness are shown in Fig. 2. The values measured at room temperature<sup>31</sup> are also indicated. The spectral fraction of those Fe atoms that belong to the amorphous interface changes for  $0 < x < 5$ . The average value of the HF distribution also changes continuously in this range, while the HF of the sextet component remains practically constant, as is shown by the respective components in Fig. 1(a). It should be noted here that all the HF distributions were restricted to the range below 33 T in order to avoid strong correlations with the crystalline sextet. It is also worth noting that in the evaluations, the close to 3 : 4 : 1 : 1 : 4 : 3 intensity ratios of the lines for both the crystalline sextets and the amorphous components provided the best fit, indicating an in-plane magnetization of the samples.

To explain the variation of the amount and average HF of the amorphous Fe-B alloy, first we set up a simple model of the sample structures. This is depicted schematically in Fig. 3. We suppose that below 5 nm nominal thickness, the Ag layer is not continuous. In the case of a continuous Ag layer ( $x = 5$  and 10), mixing of Fe and B takes place only at the bottom side of the Fe layer. However, when there is no Ag layer interleaved ( $x = 0$ ), it occurs both at the bottom and the top sides, and the bottom and top Fe-B interfaces overlap. In between these two

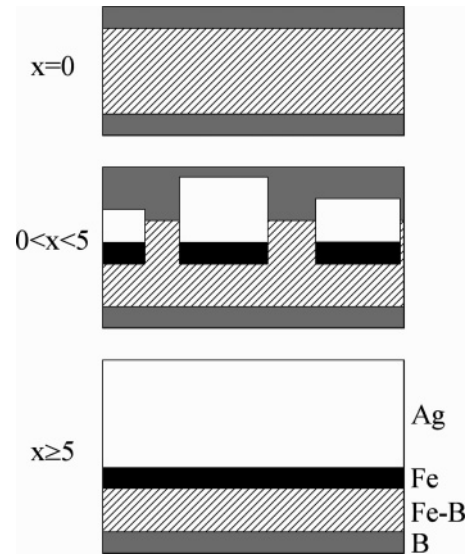


FIG. 3. Schematic sample structures formed by interface mixing in the case of different thickness of the Ag layer in the  $[2 \text{ nm B}/2 \text{ nm } ^{57}\text{Fe}/x \text{ nm Ag}]_4$  multilayer series, as inferred from the Mössbauer measurements. In the case of a continuous Ag layer ( $x \geq 5$ ), mixing of Fe and B (dashed area) takes place only at the bottom side of the Fe layer. When there is no Ag layer interleaved ( $x = 0$ ), it occurs both at the bottom and the top sides and the 2 nm Fe layer is fully amorphized. For  $0 < x < 5$ , Ag islands are formed with varying area and height and protect the top side of the underlying Fe area from amorphization.

extremes ( $0 < x < 5$ ), Ag islands are formed with varying area and height, which protect the underlying area of the Fe layer from being intermixed with the topside B layer. The area of the Ag-covered Fe layer gradually increases with  $x$ , and as a consequence the ratio of bcc Fe increases and that of the amorphous interface decreases. The presence of an unalloyed B layer—indicated by the gray layers in Fig. 3—on the one hand can be predicted from the average concentration of the amorphous layers as estimated in the following, and on the other hand could be observed by transmission electron microscopy.<sup>30</sup> (If a homogeneous amorphous phase were formed from the Fe and B layers of equal thickness, it would have 40 at. % Fe concentration and would be nonmagnetic.) The validity of the above simple model is of course limited. In the case of very small Ag islands, the lateral diffusion of Fe and B should also be taken into account, and nonequilibrium mixing of Ag with either Fe or B or with the amorphous Fe-B alloy might also take place. However, it is remarkable that both the fraction and the average HF of the amorphous phase keep varying in the small Ag thickness range too, as can be seen in Fig. 2.

According to the above model, the changes observed in the parameters of the amorphous layer as a function of the Ag layer thickness are due to the different ratio of the extent of the Fe/B interface as compared to that of the B/Fe interface. The 16 T average HF at 13 K temperature for  $x = 0$  is an average value taken over the top and the bottom interfaces containing an approximately equal number of Fe atoms. The average HF of the B/Fe interface is close to 19 T, as is revealed by the samples,  $x = 5$  and 10, where the Ag layer is continuous and forms a perfect barrier to the formation of the Fe/B interface.

If we use the parameters of cosputtered amorphous alloys,<sup>32</sup> the 19 T value belongs to a concentration around Fe<sub>59</sub>B<sub>41</sub>, and the 3 T decrease of the average HF when  $x = 0$  belongs to an about 6 at. % increase of the average B concentrations. The fact that in the case of  $x = 0$  the average is calculated over top and bottom interfaces containing an equal number of Fe atoms means that the average B concentration of the Fe/B interface is about 11 at. % higher than that of the B/Fe interface.

The HF distributions, as can be seen in Fig. 1(b), cover a broad range of field values and have a bimodal character for all the samples. (Here we note that while the two peaks below 10 T and above 20 T are well separated and reproduced when applying other evaluation methods,<sup>14</sup> the small oscillations observed in the 20–30 T range can be due to the evaluation method<sup>27</sup> based on a finite set of equidistant HF values.) The broad peak around 25 T belongs to about 30 at. % B concentration, while the low field peak belongs to regions of close to 60 at. % B concentration, where the alloy becomes nonmagnetic. The low field peak is partly due to paramagnetic components having a quadruple splitting<sup>32</sup> around 0.64 mm/s, which cannot be separated<sup>13</sup> from magnetic components of around a 3 T field. The decrease of the average HF with decreasing Ag thickness or increasing temperature is partly the result of an increase in the respective ratio of the low field components, but it is also due to a slight shift of the peak positions of the HF distributions. Since the presence of superparamagnetic relaxation could be excluded by measurements in external magnetic field,<sup>13</sup> the sharp decrease of the average HF at room temperature in the vicinity of  $x = 0$  (see Fig. 2) is largely due to the increasing weight of those components where the Curie temperature is below room temperature.

The standard deviation of the distributions in Fig. 1(b) varies between 8.6(5) and 8.8(5) T, which is much greater than in the case of melt quenched or sputtered amorphous alloys.<sup>32</sup> It is supposed to result mainly from a concentration gradient along the growth direction, which is—according to the above considerations—at least 30 at. %. Although lateral concentration fluctuations cannot be excluded, this explanation is supported by the observation of a more homogeneous amorphous layer in Fe-B multilayers<sup>14</sup> when the thickness of the Fe layer is decreased below 2 nm. It is important to note, however, that in the multitrilayers, the varying Ag thickness introduces a new source of concentration difference. When the amorphous layer is in between B and Fe layers, as is the case for  $x = 5$  and 10, there is a difference in the number of B near neighbors for Fe atoms at the bottom or at the top of the amorphous layer, i.e., at the “interface” of the interface layer. In the case of  $x = 0$ , the amorphous layer is bordered by B layers on the two sides; the bottom and top sides of the amorphous layer are symmetric in this respect. The variation observed in the HF distributions, therefore, comes not only from a varying ratio of the B/Fe and Fe/B interfaces, but to some extent from the varying neighborhood of the amorphous interface layer.

#### IV. RESULTS AND DISCUSSION OF B/Fe/B and B/Fe/Ag TRILAYERS

The examination of the trilayers, where only the cover layers are different, can answer definitively the question of

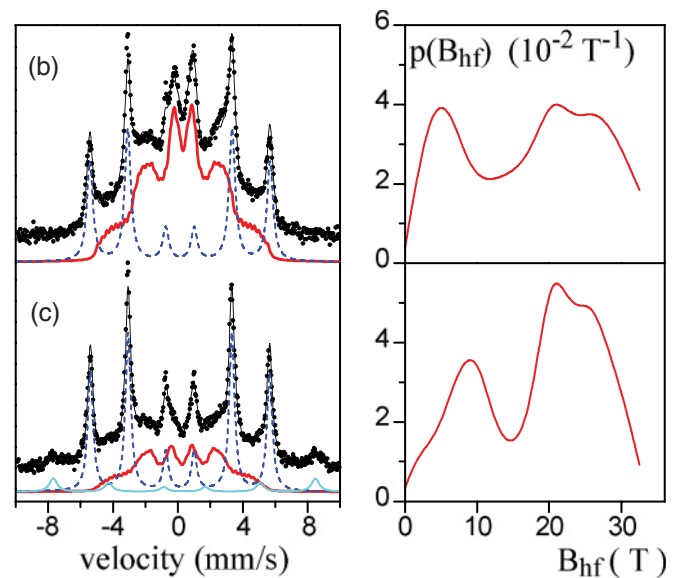


FIG. 4. (Color online) CEMS spectra measured at 15 K for the following samples: (b) Si/5 nm B/2.5 nm <sup>57</sup>Fe/5 nm B/10 nm Ag, and (c) Si/5 nm B/2.5 nm <sup>57</sup>Fe/10 nm Ag. The subspectra of the crystalline Fe layer (dashed line, blue) and the amorphous Fe-B interface (black solid line, red) are also indicated. In the case of (c), a small amount of oxide phase (gray solid line, cyan) can also be observed. The normalized hyperfine field distributions evaluated for the amorphous Fe-B interfaces are shown on the right panels. The difference of the HF distributions reveals that the Fe/B and the B/Fe interfaces are not equivalent

whether there is a difference between the B/Fe and Fe/B interfaces, and it can reveal to what extent the additional effects (variation of the sample morphology or the varying neighborhood of the amorphous interface layer) contribute to the observed difference in the case of varying layer sequence or Ag thickness. Since here the Ag layer is applied only as a cover layer, it is not supposed to affect the bottom interface of the Fe layer.

The low-temperature spectra of samples (b) and (c) are shown in Fig. 4. Similarly to the multilayer samples of Fig. 1, the spectra were described by a slightly broadened sextet [ $\Gamma = 0.45(1)$  and  $0.40(1)$  mm/s for (b) and (c), respectively] and a HF distribution. Here, as well, the sextet [HF = 34.3(2) T and 0.13(1) mm/s isomer shift for both samples] belongs to the crystalline Fe layer, while the broad HF distribution is attributed to the amorphous interfaces. [The parameters determined for sample (b) suggest that the Fe/Ag interface contribution is not the only source of the slight increase of the HF and the linewidth of the crystalline sextet, as compared to bulk  $\alpha$ -Fe.] In the case of sample (c), a small amount of oxide component (7%) is also found, which is described by a broad sextet of about 50 T magnetic splitting and 0.4 mm/s isomer shift (green subspectrum in Fig. 4). The Fe oxide is probably formed at the surface of the sample after removing it from the vacuum chamber, since there is no observable oxide phase in the thicker multilayer samples or in the case of sample (b). It seems that the 5 nm B layer is more effective in preventing the oxidation of the Fe layer than the 10 nm Ag layers, especially when it is exposed to cooling cycles.

The shape of the broad spectral component indicated by the black-solid-line (red) subspectra in Fig. 4 and described by the respective HF distribution is very different for the two samples. If top and bottom interfaces were the same, it is only the spectral ratio of this component which would be expected to change. The difference mainly comes from the enhancement of the low field components in sample (b) as compared to (c), but there is a visible shift in the position of the low field peak as well. It is around 5.1 T in sample (b) and around 9.4 T in sample (c). The variations observed in the shape of the HF distribution are very similar to what have been found for the multitrilayer samples [see Fig. 1(b)] as a function of the Ag layer thickness. The average HF of the amorphous component is 17.1(2) and 18.6(2) T for samples (b) and (c), respectively. The 1.5 T decrease of the average HF belongs to an about 3 at. % increase of the average B concentrations,<sup>32</sup> which means that the B concentration of the Fe/B interface is about 6 at. % higher than that of the B/Fe interface.

The amount of Fe atoms in the amorphous interface is equivalent to 1.7- and 1-nm-thick Fe layers for samples (b) and (c), respectively, when it is calculated from the spectral ratio of the amorphous component (69% and 39%, respectively) and the 2.5-nm nominal width of the <sup>57</sup>Fe layer. These thickness values agree quite well with those observed for the sum of the two interfaces in our previous study on Fe-B multilayers<sup>14</sup> and for the B/Fe interface discussed in the previous section or studied by sequence permutation.<sup>13</sup> This agreement is important since in this way we can exclude the

effect of intermixing with the substrate, which could modify the properties of the bottom interface. It was in fact found that the bottom interface contribution starts to decrease at around 2 nm B layer thickness, which is explained by the intermixing of B and Si.

## V. CONCLUSIONS

Mössbauer spectroscopy is a powerful method to observe and quantitatively analyze the difference between the top and bottom interfaces of nanometer-scale Fe layers. In the case of Fe-B multilayers, an amorphous interface layer is formed, and the “B on top of Fe” interface has been shown to be more B-rich than the “Fe on top of B” interface. This was established by applying layers of a third element, Ag, which does not mix with either of the two other elements and through studying three different layer arrangements: multitrilayers with different sequence of the elements,<sup>13</sup> multitrilayer samples with a fixed sequence but varying Ag layer thickness, and finally single B/Fe/Ag and B/Fe/B trilayers. The smallest B concentration difference of the top and bottom interfaces, around 6 at. %, was observed in the case of the single trilayers. In multitrilayers, the variance of the layer morphologies was shown to enhance the difference.

## ACKNOWLEDGMENTS

This work was supported by the Hungarian Scientific Research Fund (OTKA) Grant No. K 101456.

\*balogh.judit@wigner.mta.hu

- <sup>1</sup>V. M. Uzdin, A. Vega, A. Khrenov, W. Keune, V. E. Kuncser, J. S. Jiang, and S. D. Bader, *Phys. Rev. B* **85**, 024409 (2012).
- <sup>2</sup>F. Stromberg, W. Keune, V. E. Kuncser, and K. Westerholt, *Phys. Rev. B* **72**, 064440 (2005).
- <sup>3</sup>F. Gustavsson, E. Nordström, V. H. Etgens, M. Eddrief, E. Sjöstedt, and J.-M. George, *Phys. Rev. B* **66**, 024405 (2002).
- <sup>4</sup>V. M. Uzdin, W. Keune, H. Schrör, and M. Walterfang, *Phys. Rev. B* **63**, 104407 (2001).
- <sup>5</sup>R. Jungblut, R. Coehoorn, M. T. Johnson, Ch. Sauer, P. J. van der Zaag, A. R. Ball, Th.G. S. M. Rijks, J. aan de Stegge, and A. Reinders, *J. Magn. Magn. Mater.* **148**, 300 (1995).
- <sup>6</sup>S. Couet, Th. Diederich, S. Stankov, K. Schlage, T. Slezak, R. Ruffer, J. Korecki, and R. Röhlberger, *Appl. Phys. Lett.* **94**, 162501 (2009).
- <sup>7</sup>T. Shinjo and W. Keune, *J. Magn. Magn. Mater.* **200**, 598 (1999).
- <sup>8</sup>A. Gupta, D. Kumar, and V. Phatak, *Phys. Rev. B* **81**, 155402 (2010).
- <sup>9</sup>R. Gupta, M. Weisheit, H.-U. Krebs, and P. Schaaf, *Phys. Rev. B* **67**, 075402 (2003).
- <sup>10</sup>A. Gupta, M. Gupta, S. Chakravarty, R. Ruffer, H.-C. Wille, and O. Leupold, *Phys. Rev. B* **72**, 014207 (2005).
- <sup>11</sup>D. G. Merkel, Sz. Sajti, Cs. Fetzter, J. Major, M. Major, R. Ruffer, A. Rühm, S. Stankov, F. Tanczikó, and L. Bottyán, *J. Phys.: Conf. Ser.* **211**, 012029 (2010).
- <sup>12</sup>O. Marks, T. Ruckert, J. Tappert, W. Keune, W.-S. Kim, W. Kleemann, and J. Voiron, *IEEE Trans. Magn.* **34**, 834 (1998).
- <sup>13</sup>J. Balogh, L. Bujdosó, D. Kaptás, T. Kemény, I. Vincze, A. Kovács, and L. Tóth, *J. Appl. Phys.* **105**, 104303 (2009).

- <sup>14</sup>J. Balogh, L. Bujdosó, T. Kemény, T. Pusztai, L. Tóth, and I. Vincze, *Appl. Phys. A* **65**, 23 (1997).
- <sup>15</sup>R. Steiner, H. G. Boyen, M. Krieger, A. Plettl, P. Widmayer, P. Ziemann, F. Banhart, R. Kilper, and P. Oelhafen, *Appl. Phys. A* **76**, 5 (2003).
- <sup>16</sup>M. Neubauer, K. P. Lieb, P. Schaaf, and M. Uhrmacher, *Phys. Rev. B* **53**, 10237 (1996).
- <sup>17</sup>P. J. Schurer, Z. Celinski, and B. Heinrich, *Phys. Rev. B* **51**, 2506 (1995).
- <sup>18</sup>J. Korecki and U. Gradmann, *Phys. Rev. Lett.* **55**, 2491 (1985).
- <sup>19</sup>J. Balogh, L. Bujdosó, T. Kemény, and I. Vincze, *J. Phys.: Condens. Matter* **9**, L503 (1997).
- <sup>20</sup>I. N. Mastorakos, H. M. Zbib, and D. F. Bahr, *Appl. Phys. Lett.* **94**, 173114 (2009).
- <sup>21</sup>S. Roy and B. N. Dev, *Appl. Surf. Sci.* **257**, 7566 (2011).
- <sup>22</sup>M. Arend, M. Finazzi, O. Schulte, M. Münzenberg, A.-M. Dias, F. Baudelet, C. Giorgetti, E. Dartyge, P. Schaaf, J.-P. Kappler, G. Krill, and W. Felsch, *Phys. Rev. B* **57**, 2174 (1998).
- <sup>23</sup>M. Pakala, Y. Huai, G. Anderson, and L. Miloslavsky, *J. Appl. Phys.* **87**, 6653 (2000).
- <sup>24</sup>R. Ranchal, C. Aroca, M. C. Sánchez, P. Sánchez, and E. López, *Appl. Phys. A* **82**, 697 (2006).
- <sup>25</sup>A. N. Pogorily, G. V. Bondarkova, O. N. Razumov, and E. V. Shypil, *J. Appl. Phys.* **109**, 07C118 (2011).
- <sup>26</sup>K. Fukumura, A. Nakanishi, and T. Kobayashi, *Nucl. Instrum. Methods Phys. Res., Sect. B* **86**, 386 (1994).
- <sup>27</sup>J. Hesse and A. Rübartsch, *J. Phys. E* **7**, 526 (1974).

- <sup>28</sup>I. Dézsi, Cs. Fetzer, I. Szücs, B. Degroote, A. Vantomme, T. Kobayashi, and A. Nakanishi, *Surf. Sci.* **601**, 2525 (2007).
- <sup>29</sup>J. Balogh, D. Kaptás, I. Vincze, K. Temst, and C. Van Haesendonck, *Phys. Rev. B* **76**, 052408 (2007).
- <sup>30</sup>L. F. Kiss, J. Balogh, L. Bujdosó, D. Kaptás, T. Kemény, A. Kovács, and I. Vincze, *J. Alloys Compd.* **509**, S188 (2011).
- <sup>31</sup>J. Balogh, L. Bujdosó, D. Kaptás, L. F. Kiss, T. Kemény, and I. Vincze, *J. Phys.: Conf. Ser.* **217**, 012089 (2010).
- <sup>32</sup>G. Xiao and C. L. Chien, *Phys. Rev. B* **35**, 8763 (1987).